Transport of ultracold Bose gases beyond the Gross-Pitaevskii description

Thomas Ernst,[1] Tobias Paul,[2] and Peter Schlagheck[3,4,*]

[1]*Centre for Theoretical Chemistry and Physics and Institute of Natural Sciences, Massey University, Auckland 0745, New Zealand*

[2]*Institut für Theoretische Physik, Universität Heidelberg, D-69120 Heidelberg, Germany*

[3]*Institut für Theoretische Physik, Universität Regensburg, D-93040 Regensburg, Germany*

[4]*Mathematical Physics, Lund Institute of Technology, S-22100 Lund, Sweden*

(Received 28 May 2009; published 29 January 2010)

We explore atom-laser-like transport processes of ultracold Bose-condensed atomic vapors in mesoscopic waveguide structures beyond the Gross-Pitaevskii mean-field theory. Based on a microscopic description of the transport process in the presence of a coherent source that models the outcoupling from a reservoir of perfectly Bose-Einstein condensed atoms, we derive a system of coupled quantum evolution equations that describe the dynamics of a dilute condensed Bose gas in the framework of the Hartree-Fock–Bogoliubov approximation. We apply this method to study the transport of dilute Bose gases through an atomic quantum dot and through waveguides with disorder. Our numerical simulations reveal that the onset of an explicitly time-dependent flow corresponds to the appearance of strong depletion of the condensate on the microscopic level and leads to a loss of global phase coherence.

DOI: 10.1103/PhysRevA.81.013631 PACS number(s): 03.75.Kk, 03.75.Pp, 67.85.De

I. INTRODUCTION

The rapid progress in the experimental techniques for trapping and manipulating ultracold Bose gases on microscopic scales has opened the possibility for investigating mesoscopic transport properties with interacting bosonic matter waves. A key achievement in this context is the development of simple or more complex waveguide geometries for cold atoms with optical techniques (as, e.g., in Ref. [1]) or with atom chips [2–4], which also allow one to impose scattering and disorder potentials on microscopic scales (e.g., [5,6]) and which also permit one to detect individual atoms with rather good accuracy [7]. Coherent transport processes in such waveguides, where the atoms of the Bose gas are freely propagating along the guide with some finite momentum, can be studied, on the one hand, through bosonic wave packets that are created upon sudden release of a Bose-Einstein condensate from a trap, which is then accelerated in the presence of a finite potential gradient along the guide [8,9]. On the other hand, the principle of an atom laser [10,11] can be used for this purpose, as was recently demonstrated in Refs. [12–15]. In these experiments, a coherent matter-wave beam was injected from a Bose-Einstein condensate in a trap into an optical waveguide. This was achieved by means of a radio-frequency (rf)-induced transition from a magnetically trapped ($m_F = -1$) to an untrapped ($m_F = 0$) hyperfine state of ^{87}Rb in Ref. [12,13], and by means of a careful ramping of a magnetic-field gradient in an optical trap in Ref. [15]. In this way, it becomes possible to study bosonic scattering processes with cold atoms at well-defined incident energy, in close analogy to scattering of laser beams and to electronic transport in mesoscopic solid-state systems [16].

From the theoretical side, a number of investigations on the quasicontinuous transport of ultracold Bose gases and Bose-Einstein condensates have been undertaken during the past decade. This started with the attempt to define an atomic analog of Landauer's quantization of conductance [17] and was continued by first investigations of nonlinear resonant transport and interaction blockade in quantum-dot-like scattering potentials [18,19]. Propagation and transmission studies were then undertaken on the basis of the stationary Gross-Pitaevskii equation [20–23] as well as through a time-dependent integration approach in which the injection of bosonic matter waves was accounted for by means of a coherent source term [24–26].

With few exceptions (e.g., Ref. [19]), the above studies were mainly based on an effective one-dimensional Gross-Pitaevskii equation. This implicitly assumes the realization of a one-dimensional mean-field regime [27] where the transverse confinement of the waveguide is strong enough to inhibit the population of transversally excited modes, but not so strong as to come close to the Tonks-Girardeau regime of impenetrable atoms [28,29]. Furthermore, the phase coherence length for a freely propagating atomic beam, which is generally finite for one-dimensional quasicondensates [30], is assumed to be considerably larger than the effective longitudinal extent of the waveguide (which may be limited due to a finite focal region in the case of an elongated dipole guide [12], or due to atom detection [7]). Using the one-dimensional Gross-Pitaevskii equation under these conditions, the presence of atom-atom interaction in the bosonic beam mainly manifests, as in nonlinear optics [31], in finite nonlinearity effects in the wave scattering process, such as nonlinearity-induced shifts of resonant transmission peaks [18,22,24].

The main focus of this work is to determine the quantitative amount of *depletion* that is generated during the transport process of the condensate, which is rather relevant information from the experimental point of view. Indeed, too much depletion would eventually lead to a complete destruction of the phase coherence of the beam, which means that wave interference phenomena in the transport process, which would result from the coherent Gross-Pitaevskii equation, may, in this case, not be observable in practice. Inspired by previous studies [32–34], we use a quantum kinetic approach for this purpose, which is equivalent to the Hartree-Fock–Bogoliubov

*Present address: Département de Physique, Université de Liège, 4000 Liège, Belgium.

approximation [35]. In practice, the condensate wave function is, in this approach, propagated together with two-component functions that describe the coherence as well as the one-body density matrix associated with noncondensed atoms. This ansatz generally involves a renormalization of the microscopic interaction strength, which, however, does not represent a conceptual problem in the quasi-one-dimensional confinement geometries that we are considering here. Moreover, it explicitly breaks the gauge symmetry of the Bose gas and introduces a gap in the excitation spectrum [34–36]. We justify this due to the fact that the matter-wave beam is, in the guided atom-laser scenario, connected to an idealized reservoir that contains a macroscopically large Bose-Einstein condensate, for which spontaneous breaking of gauge symmetry can be well assumed [37].

In order to provide a solid theoretical foundation of our approach, we begin, in Sec. II, with a step-by-step derivation of the quantum kinetic equations that are used to model the propagation process of the condensate in the presence of depletion. For the sake of definiteness, we focus here on an atom-laser process that is based on the rf-induced outcoupling of atoms from a Bose-Einstein condensate in a magnetic trap [12,13]. Our starting point is the microscopic many-body description of the two-component system that defines this atom laser, from which we derive, under the assumption of a weak effective atom-atom interaction in the waveguide, nonlinear kinetic equations for the condensate wave function and for two-component functions that account, in lowest order, for quantum depletion. In Secs. III and IV, respectively, we apply this approach to transport processes of Bose-Einstein condensates through double barrier potentials and disorder potentials that were also studied in Refs. [24,25] on the basis of the Gross-Pitaevskii equation. Our main finding, which is summarized in the conclusion in Sec. V, is that the overall coherence of the atomic beam remains fairly well preserved over reasonably long time scales in the case of a quasistationary flow of the condensate, while strong depletion arises in the case of permanently time-dependent scattering in the waveguide.

II. KINETIC EQUATIONS FOR THE SCATTERING SYSTEM

We consider a gas of ultracold bosonic atoms that are confined in a large trap and injected from there into a mesoscopic waveguide structure (see Fig. 1). In practice, such a "guided atom laser" can be realized by combining a magnetic trapping potential with an optical waveguide which is, for example, created by an elongated dipole trap. A radio-frequency field is then used to flip the spins of the atoms and induce coherent transitions from a low-field seeker state $|r\rangle$ (such as the $|F, m_F\rangle = |1, -1\rangle$ state of ^{87}Rb) to a hyperfine state $|g\rangle$ that is, in lowest order, insensitive to the magnetic field (the $|F, m_F\rangle = |0, 0\rangle$ state of ^{87}Rb) but still experiences the optical potential. As demonstrated in Refs. [12,13] where this setup was experimentally realized, the quadratic Zeeman effect can be exploited to compensate the quadratic variation of the laser intensity along the dipole trap and to thereby create a rather homogeneous waveguide potential.

In the formalism of second quantization, the quantum dynamics of this two-component system is described by the

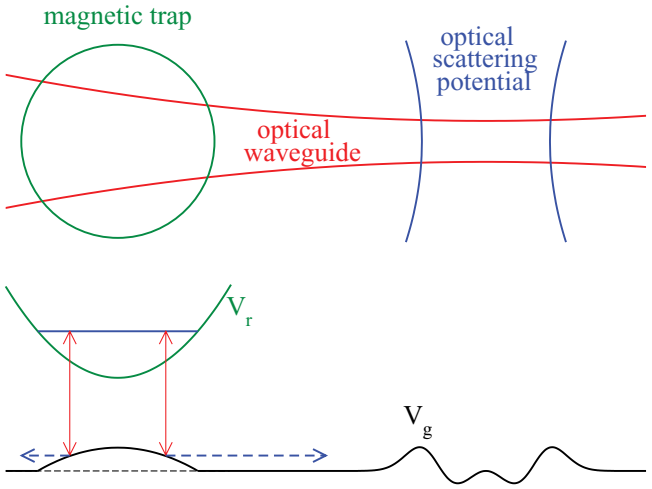

FIG. 1. (Color online) Possible waveguide geometry for a guided atom-laser experiment with Bose-Einstein condensates in the presence of an optical scattering potential. The lower panel shows the effective potentials along the longitudinal coordinate x for the reservoir (V_r, green parabola) and the waveguide atoms (V_g, black horizontal curve). A radio-frequency field with suitable frequency $\omega_{\rm rf}$ (indicated by the vertical red line) can be used to resonantly couple atoms from the trapped condensate (whose chemical potential is denoted by the horizontal blue line) into the waveguide.

coupled equations

$$
\begin{aligned}
i\hbar\frac{\partial}{\partial t}\hat{\Psi}_g(\mathbf{r},t) &= \left(-\frac{\hbar^2}{2m}\Delta + V_g(\mathbf{r})\right)\hat{\Psi}_g(\mathbf{r},t) \\
&\quad + U_g\hat{\Psi}_g^\dagger(\mathbf{r},t)\hat{\Psi}_g(\mathbf{r},t)\hat{\Psi}_g(\mathbf{r},t) \\
&\quad + U_{rg}\hat{\Psi}_r^\dagger(\mathbf{r},t)\hat{\Psi}_r(\mathbf{r},t)\hat{\Psi}_g(\mathbf{r},t) \\
&\quad + K(t)\hat{\Psi}_r(\mathbf{r},t) \qquad (1) \\
i\hbar\frac{\partial}{\partial t}\hat{\Psi}_r(\mathbf{r},t) &= \left(-\frac{\hbar^2}{2m}\Delta + V_r(\mathbf{r})\right)\hat{\Psi}_r(\mathbf{r},t) \\
&\quad + U_r\hat{\Psi}_r^\dagger(\mathbf{r},t)\hat{\Psi}_r(\mathbf{r},t)\hat{\Psi}_r(\mathbf{r},t) \\
&\quad + U_{rg}\hat{\Psi}_g^\dagger(\mathbf{r},t)\hat{\Psi}_g(\mathbf{r},t)\hat{\Psi}_r(\mathbf{r},t) \\
&\quad + K^*(t)\hat{\Psi}_g(\mathbf{r},t), \qquad (2)
\end{aligned}
$$

for the bosonic field operators $\hat{\Psi}_g(\mathbf{r},t)$ and $\hat{\Psi}_r(\mathbf{r},t)$ that annihilate atoms in the "waveguide state" $|g\rangle$ and the "reservoir state" $|r\rangle$, respectively. $V_g(\mathbf{r})$ denotes the waveguide potential while $V_r(\mathbf{r})$ corresponds to the magnetic trap (perturbed by the presence of the optical guide) that confines the reservoir atoms in the state $|r\rangle$. The short-range interaction between the atoms in the involved hyperfine states is represented by contact potentials of the form $U(\mathbf{r}_1 - \mathbf{r}_2) \propto \delta(\mathbf{r}_1 - \mathbf{r}_2)$ with the prefactors U_g, U_r, and U_{rg} for $|g\rangle$-$|g\rangle$, $|r\rangle$-$|r\rangle$, and $|g\rangle$-$|r\rangle$ interaction processes, respectively. Transitions between waveguide and reservoir states are induced by the coupling amplitude $K(t)$, which is adiabatically raised from zero to a finite value and which would correspond to the field strength of the rf radiation.

It is reasonable from the experimental point of view to consider an initial many-body state in the trap that consists of a nearly perfect Bose-Einstein condensate containing a rather large number of atoms. Provided the coupling amplitude $K(t)$

is not too strong, we can safely assume that the condensate is not appreciably affected by the outcoupling process on finite time scales. We therefore make the ansatz

$$\hat{\Psi}_r(\mathbf{r},t) = \langle \hat{\Psi}_r(\mathbf{r},t)\rangle = \Psi_r(\mathbf{r})\exp(-i\mu t/\hbar), \tag{3}$$

where $\Psi_r(\mathbf{r})$ is the macroscopically populated condensate wave function that satisfies the Gross-Pitaevskii equation

$$\left(-\frac{\hbar^2}{2m}\Delta + V_r(\mathbf{r}) + U_r|\Psi_r(\mathbf{r})|^2\right)\Psi_r(\mathbf{r}) = \mu\Psi_r(\mathbf{r}), \tag{4}$$

with the normalization

$$\int d^3r|\Psi_r(\mathbf{r})|^2 = \mathcal{N}_r \gg 1, \tag{5}$$

and μ denotes the chemical potential of the condensate. This ansatz explicitly involves a spontaneous breaking of the condensate's gauge symmetry, which should be valid in the thermodynamic limit of a very large number $\mathcal{N}_r$ of atoms in the trap [37]. It furthermore neglects the presence of noncondensed atoms in the trap. Inserting this expression for $\hat{\Psi}_r(\mathbf{r},t)$ into Eq. (1) yields then

$$\begin{aligned} i\hbar\frac{\partial}{\partial t}\hat{\Psi}_g(\mathbf{r},t) = &\left[-\frac{\hbar^2}{2m}\Delta + V_g(\mathbf{r}) + U_{rg}|\Psi_r(\mathbf{r})|^2\right]\hat{\Psi}_g(\mathbf{r},t) \\ &+ U_g\hat{\Psi}_g^\dagger(\mathbf{r},t)\hat{\Psi}_g(\mathbf{r},t)\hat{\Psi}_g(\mathbf{r},t) \\ &+ K(t)\Psi_r(\mathbf{r})\exp(-i\mu t/\hbar), \end{aligned} \tag{6}$$

as the equation for the field operator of the waveguide state, which contains a coherent source term with the amplitude $K(t)\Psi_r(\mathbf{r})$.

The external potential for the atoms in the state $|g\rangle$ is written as

$$V_g(\mathbf{r}) = \tfrac{1}{2}m\omega_\perp^2 r_\perp^2 + V(x), \tag{7}$$

where x and $\mathbf{r}_\perp \equiv (y,z)$ denote the spatial coordinates along and perpendicular to the waveguide, respectively, and $\omega_\perp$ is the transverse confinement frequency. In addition to the waveguide, we consider the presence of a longitudinal scattering potential $V(x)$ of finite spatial range, which could, for example, be a sequence of barriers or speckle disorder induced by other laser fields. Denoting the transverse eigenstates within the waveguide by $\chi_n(\mathbf{r}_\perp)$, we can make the decomposition $\hat{\Psi}_g(\mathbf{r},t) = \sum_n \chi_n(\mathbf{r}_\perp)\hat{\psi}_n(x,t)$ for the field operator of the $|g\rangle$-atoms, where $\hat{\psi}_n(x,t)$ annihilates a particle at position x in the nth transverse eigenmode. This decomposition can be generalized for waveguides with confinement frequencies $\omega_\perp$ that are slowly varying with the longitudinal coordinate x; in that case, the eigenstates $\chi_n(\mathbf{r}_\perp)$ would vary with x as well, through their parametric dependence on $\omega_\perp$ [38].

In general, the coherent source in Eq. (6) populates a finite linear combination of transverse eigenmodes in the waveguide, which would be coupled to each other through the interaction term. Clean bosonic scattering experiments, however, would ideally require a well-defined longitudinal kinetic energy of the atoms, which means that the population ought to be restricted to one single transverse mode. Technically, this task could possibly be accomplished by imposing a smooth barrier potential along the waveguide with a maximum height $V_{\max}$ that satisfies $\mu - 2\hbar\omega_\perp < V_{\max} < \mu - \hbar\omega_\perp$. In this case, atoms in the transverse ground mode (with the offset energy $\hbar\omega_\perp$) would have just enough kinetic energy to pass that barrier, while components associated with excited transverse modes (with offset energies $\geqslant 2\hbar\omega_\perp$) would be reflected. Ideally, the scattering region described by the potential $V(x)$ would then have to be defined near the top of that barrier (provided the latter is broad enough) in order to minimize the loss of population into transversally excited states due to the presence of the interaction.

In the following, we assume that the population of the waveguide by the source can indeed be restricted to the transverse ground mode $\chi_0(\mathbf{r}_\perp) \propto \exp(-m\omega_\perp r_\perp^2/2\hbar)$. We then make the simplifying ansatz

$$\hat{\Psi}_g(\mathbf{r},t) = \chi_0(\mathbf{r}_\perp)\hat{\psi}(x,t), \tag{8}$$

which restricts the consideration to this ground mode and neglects the effect of (possibly virtual) transitions to excited transverse modes due to the interaction. $\hat{\psi}(x,t)$ then satisfies the equation

$$\begin{aligned} i\hbar\frac{\partial}{\partial t}\hat{\psi}(x,t) = &H_0^{(x)}\hat{\psi}(x,t) + g\hat{\psi}^\dagger(x,t)\hat{\psi}(x,t)\hat{\psi}(x,t) \\ &+ S(x,t)\exp(-i\mu t/\hbar), \end{aligned} \tag{9}$$

with the one-dimensional single-particle Hamiltonian

$$H_0^{(x)} = -\frac{\hbar^2}{2m}\frac{\partial^2}{\partial x^2} + V(x) + \hbar\omega_\perp, \tag{10}$$

and the effective one-dimensional interaction strength

$$g = \frac{m\omega_\perp}{2\pi\hbar}U_g = 2\hbar\omega_\perp a_s, \tag{11}$$

where a_s is the s-wave scattering length for atoms in the state $|g\rangle$. The source amplitude in this one-dimensional equation is given by

$$S(x,t) = \int d^2r_\perp \chi_0^*(\mathbf{r}_\perp)\Psi_r(\mathbf{r})K(t). \tag{12}$$

Assuming that the condensate wave function $\Psi_r(\mathbf{r})$ has no overlap with the region in which the scattering potential $V(x)$ is defined, we make in the following the idealized ansatz of a strongly localized source, namely

$$S(x,t) = S_0(t)\delta(x - x_0), \tag{13}$$

where x_0 corresponds to the position around which the trap is centered.

Our aim is to compute the time evolution of the condensate wave function in the waveguide as well as the amount of depletion that is generated during this transport process. To this end, we follow the lines of the treatment in Refs. [32,33] and make the Bogoliubov ansatz for the field operator $\hat{\psi}(x,t)$ in the transverse ground mode of the waveguide, which is decomposed into its order parameter $\langle\hat{\psi}(x,t)\rangle$ and a quantum fluctuation operator $\delta\hat{\psi}(x,t)$ according to

$$\hat{\psi}(x,t) = \langle\hat{\psi}(x,t)\rangle + \delta\hat{\psi}(x,t). \tag{14}$$

Using Eq. (9), it is then straightforward to derive an infinite set of coupled kinetic equations for the condensate wave function $\langle\hat{\psi}(x,t)\rangle$ and the expectation values of products of the operators $\delta\hat{\psi}(x,t)$ and their Hermitean conjugates—that is for the n-point functions $\langle\delta\hat{\psi}(x_1,t)\delta\hat{\psi}(x_2,t)\rangle$, $\langle\delta\hat{\psi}^\dagger(x_1,t)\delta\hat{\psi}(x_2,t)\rangle$,

$\langle\delta\hat{\psi}(x_1,t)\delta\hat{\psi}(x_2,t)\delta\hat{\psi}(x_3,t)\rangle$, etc. The time evolution of $\langle\hat{\psi}(x,t)\rangle$, for instance, is described by the equation

$$\begin{aligned} i\hbar\frac{\partial}{\partial t}\langle\hat{\psi}(x,t)\rangle &= H_0^{(x)}\langle\hat{\psi}(x,t)\rangle + g|\langle\hat{\psi}(x,t)\rangle|^2\langle\hat{\psi}(x,t)\rangle \\ &+ 2g\langle\delta\hat{\psi}^\dagger(x,t)\delta\hat{\psi}(x,t)\rangle\langle\hat{\psi}(x,t)\rangle \\ &+ g\langle\delta\hat{\psi}(x,t)\delta\hat{\psi}(x,t)\rangle\langle\hat{\psi}^\dagger(x,t)\rangle \\ &+ g\langle\delta\hat{\psi}^\dagger(x,t)\delta\hat{\psi}(x,t)\delta\hat{\psi}(x,t)\rangle \\ &+ S(x,t)\exp(-i\mu t/\hbar), \end{aligned} \tag{15}$$

which contains couplings to n-point functions up to $n=3$. The equations for the higher-order cumulants, for example, for $\langle\delta\hat{\psi}(x_1,t)\delta\hat{\psi}(x_2,t)\rangle$, are obtained by the time derivative of $\delta\hat{\psi}(x,t)\equiv\hat{\psi}(x,t)-\langle\hat{\psi}(x,t)\rangle$ through the combination of Eqs. (9) and (15).

In order to define a meaningful truncation scheme for this infinite hierarchy of equations, we make the standard mean-field assumption that we have a rather small interaction strength g, corresponding to a small s-wave scattering length a_s of the atoms in the waveguide, and a comparatively large source amplitude S_0, giving rise to a large longitudinal density $n_0=(m/2\mu)|S_0/\hbar|^2$ of atoms that are injected by the source. The mean-field regime could then be expressed by the inequalities $n_0\lambda\gg 1$ and $a_s/\lambda\ll 1$ where λ characterizes the relevant length scales of the waveguide system [such as the transverse oscillator length $a_\perp=\sqrt{\hbar/m\omega_\perp}$, the de Broglie wavelength of the incident matter-wave beam, or the length scales introduced by the scattering potential $V(x)$]. Formally, it would be defined by the simultaneous limits $n_0\to\infty$ and $a_s\to 0$ with $a_s n_0$ remaining constant [39].

This formal mean-field limit allows us now to classify the individual terms in Eq. (15) and in the equations for the higher-order n-point functions according to different powers in the large parameter $N\equiv n_0\lambda$ characterizing the number of atoms within the length scale λ. As we have $|S_0|=\hbar\sqrt{2\mu n_0/m}\propto\sqrt{N}$, we can obviously infer from Eq. (15) that the condensate wave function $\langle\hat{\psi}(x,t)\rangle$ scales as $O(N^{1/2})$ for finite evolution times. The equation for $\langle\delta\hat{\psi}(x_1,t)\delta\hat{\psi}(x_2,t)\rangle$ [see Eq. (20) below] is not directly connected to the coherent source, but contains the inhomogeneous term $g\delta(x_1-x_2)\langle\hat{\psi}(x_1,t)\rangle\langle\hat{\psi}(x_2,t)\rangle$ through which this two-point function becomes populated in the course of time evolution. Taking into account that $g\propto 1/N$ in this formal mean-field limit and using $\langle\hat{\psi}(x,t)\rangle\sim O(N^{1/2})$, we then obtain $\langle\delta\hat{\psi}(x_1,t)\delta\hat{\psi}(x_2,t)\rangle\sim O(N^0)$. Similarly one can show $\langle\delta\hat{\psi}^\dagger(x_1,t)\delta\hat{\psi}(x_2,t)\rangle\sim O(N^0)$ as well, while three-point functions such as $\langle\delta\hat{\psi}(x_1,t)\delta\hat{\psi}(x_2,t)\delta\hat{\psi}(x_3,t)\rangle$ would scale as $O(N^{-1/2})$.

Following the notation introduced by Köhler and Burnett [33], we define the condensate wave function

$$\psi(x,t)\equiv\langle\hat{\psi}(x,t)\rangle, \tag{16}$$

for atoms in the transverse ground mode of the waveguide, the pair function

$$\Phi(x_1,x_2,t)\equiv\langle\delta\hat{\psi}(x_2,t)\delta\hat{\psi}(x_1,t)\rangle, \tag{17}$$

and the one-body density matrix of noncondensed atoms

$$\Gamma(x_1,x_2,t)\equiv\langle\delta\hat{\psi}^\dagger(x_2,t)\delta\hat{\psi}(x_1,t)\rangle. \tag{18}$$

By taking into account all terms that scale at least as $O(N^{-1})$, we obtain a closed system of coupled equations for $\psi(x,t)$, $\Phi(x_1,x_2,t)$, and $\Gamma(x_1,x_2,t)$, namely

$$\begin{aligned} i\hbar\frac{\partial}{\partial t}\psi(x,t) &= H_0^{(x)}\psi(x,t) + g\,|\psi(x,t)|^2\,\psi(x,t) + S(x,t)\exp(-i\mu t/\hbar) && [O(N^{1/2})] \\ &+ 2g\psi(x,t)\Gamma(x,x,t) + g\psi^*(x,t)\Phi(x,x,t) && [O(N^{-1/2})] \end{aligned} \tag{19}$$

$$\begin{aligned} i\hbar\frac{\partial}{\partial t}\Phi(x_1,x_2,t) &= \left[H_0^{(x_1)} + 2g\left|\psi(x_1,t)\right|^2 + H_0^{(x_2)} + 2g\left|\psi(x_2,t)\right|^2\right]\Phi(x_1,x_2,t) \\ &+ g\delta(x_1-x_2)\psi(x_1,t)\psi(x_2,t) + g\psi^2(x_2,t)\Gamma(x_1,x_2,t) + g\psi^2(x_1,t)\Gamma(x_2,x_1,t) && [O(N^0)] \\ &+ g\delta(x_1-x_2)\Phi(x_1,x_2,t) + 2g[\Gamma(x_1,x_1,t)+\Gamma(x_2,x_2,t)]\Phi(x_1,x_2,t) \\ &+ g\Gamma(x_2,x_1,t)\Phi(x_1,x_1,t) + g\Gamma(x_1,x_2,t)\Phi(x_2,x_2,t) && [O(N^{-1})] \end{aligned} \tag{20}$$

$$\begin{aligned} i\hbar\frac{\partial}{\partial t}\Gamma(x_1,x_2,t) &= \left[H_0^{(x_1)} + 2g\left|\psi(x_1,t)\right|^2 - H_0^{(x_2)} - 2g\left|\psi(x_2,t)\right|^2\right]\Gamma(x_1,x_2,t) \\ &+ g\psi^2(x_1,t)\Phi^\star(x_1,x_2,t) - g[\psi^\star(x_2,t)]^2\Phi(x_1,x_2,t) && [O(N^0)] \\ &+ 2g[\Gamma(x_1,x_1,t)-\Gamma(x_2,x_2,t)]\Gamma(x_1,x_2,t) + g\Phi^\star(x_1,x_2,t)\Phi(x_1,x_1,t) \\ &- g\Phi(x_1,x_2,t)\Phi^\star(x_2,x_2,t), && [O(N^{-1})] \end{aligned} \tag{21}$$

where consistently all couplings to higher-order n-point functions [which would scale as $O(N^{-3/2})$ in Eq. (19) and as $O(N^{-2})$ in Eqs. (20) and (21)] are omitted.

This set of kinetic equations is equivalent to the second-order Hartree-Fock–Bogoliubov approximation in modal form [35]. It is norm conserving, that is for $x\neq x_0$ the continuity equation,

$$\frac{\partial}{\partial t}n(x,t)+\frac{\partial}{\partial x}j(x,t)=0, \tag{22}$$

is satisfied with

$$n(x,t) \equiv \langle \hat{\psi}^\dagger(x,t)\hat{\psi}(x,t)\rangle = |\psi(x,t)|^2 + \Gamma(x,x,t), \tag{23}$$

the longitudinal particle density, and

$$\begin{aligned} j(x,t) &\equiv \frac{\hbar}{2mi}\left(\frac{\partial}{\partial x_1}-\frac{\partial}{\partial x_2}\right)\langle\hat{\psi}^\dagger(x_2,t)\hat{\psi}(x_1,t)\rangle\Big|_{x_1=x_2=x} \\ &= \frac{\hbar}{2mi}\left[\psi^*(x,t)\frac{\partial}{\partial x}\psi(x,t) - \psi(x,t)\frac{\partial}{\partial x}\psi^*(x,t) \right. \\ &\quad \left. + \left(\frac{\partial}{\partial x_1}-\frac{\partial}{\partial x_2}\right)\Gamma(x_1,x_2)\Big|_{x_1=x_2=x}\right], \end{aligned} \tag{24}$$

the atomic current along the waveguide. As for the density $n(x,t)$, the current $j(x,t)$ consists of a coherent component associated with the condensate and an incoherent component that represents the noncondensed fraction, given by the second and third line of Eq. (24), respectively.

The transmission of a scattering state that is associated with a given source amplitude S_0 is obtained by dividing $j(x,t)$ through the incident current j_i. The latter is defined as the current that would be obtained at the same source amplitude S_0 if both the scattering potential $V(x)$ and the interaction strength g were zero. We straightforwardly obtain for that case the asymptotic solution

$$\psi(x,t) = -\frac{iS_0}{\hbar}\sqrt{\frac{m}{2\mu}}\exp\left[\frac{i}{\hbar}(\sqrt{2m\mu}|x-x_0|-\mu t)\right], \tag{25}$$

which yields

$$j_i = \left|\frac{S_0}{\hbar}\right|^2\sqrt{\frac{m}{2\mu}}. \tag{26}$$

We point out that the interaction strength g is assumed to vanish at $x = x_0$, which avoids effects of nonlinear backaction with the source. In between the source and the scattering potential, g is adiabatically increased with x up to a given maximal value, which remains then constant along the support of $V(x)$. Specifically, we incorporate the ramping

$$g(x) = \tfrac{1}{2}\{1+\tanh[\kappa(x-x_1)]\}\,g \tag{27}$$

of the interaction strength, where κ and x_1 are chosen such that $g(x_0) < 0.01g$ at the position x_0 of the source and $g(x) > 0.99g$ within the spatial region in which the scattering potential $V(x)$ is finite. We verified that the presence of this ramping does not cause a significant additional amount of reflection.

For the numerical treatment of the kinetic Eqs. (19)–(21), we employ a finite-difference representation of the one- and two-point functions $\psi(x,t)$, $\Phi(x_1,x_2,t)$, and $\Gamma(x_1,x_2,t)$ [26]. The numerical integration of the resulting vectorial differential equations of the form $i\dot{\mathbf{y}} = \mathcal{H}\mathbf{y}$ is then performed by means of the Crank-Nicolson method [40], which utilizes matrix-vector products as well as the solution of linear matrix-vector equations involving the effective Hamiltonian matrix $\mathcal{H}$. The split-operator technique is applied in the equations for Φ and Γ in order to do separate propagation steps in the x_1 and x_2 coordinates. To account for the nonlinearities, that is the dependence of $\mathcal{H}$ on $\mathbf{y}$, each integration step is "corrected" by repeating it with $\mathcal{H}$ being evaluated at $[\mathbf{y}(t)+\mathbf{y}^{(1)}(t+\delta t)]/2$ where $\mathbf{y}^{(1)}(t+\delta t)$ denotes the first-order estimate for $\mathbf{y}(t+\delta t)$ [26,41].

In this grid representation, the Dirac δ functions appearing in the source term (13) and in the interaction [cf. the second line of Eq. (20)] are naturally replaced by Kronecker δ's with the appropriate prefactors. We verified that the regularization of the interaction potential by a narrow Gaussian function does not significantly change our numerical results. The amplitude of the source is adiabatically ramped from zero to S_0 within $0 \leqslant t \leqslant t_0$ according to

$$S_0(t) = \sin\left(\frac{\pi}{2}\frac{t}{t_0}\right). \tag{28}$$

To avoid artificial backreflection of atoms from the boundaries of the numerical grid, we furthermore introduce complex absorbing potentials of the form $V_{\rm abs}(x) = -i\gamma(x)$ where $\gamma(x)$ is vanishing throughout the scattering region and adiabatically ramped to a finite positive value in the vicinity of the boundaries [42,43]. As the single-particle Hamiltonian of the system thereby becomes non-Hermitean, care is required for the inclusion of this imaginary potential into the equation of the one-body density matrix $\Gamma(x_1,x_2)$; we obtain $-i[\gamma(x)+\gamma(y)]\Gamma(x,y,t)$ as an additional term in Eq. (21).

III. TRANSPORT THROUGH DOUBLE BARRIER POTENTIALS

Let us first investigate resonant transport of a Bose-Einstein condensate through a symmetric double barrier potential, which can be interpreted as a Fabry-Perot resonator for coherent matter waves [18,19]. Such an atomic quantum dot may exhibit long-lived quasibound eigenstates that allow for perfect transmission at energies in the immediate vicinity of the eigenenergies of such states, while off-resonant components of the incident wave will undergo reflection. In the context of guided atom lasers, such double barrier potentials may therefore serve as tools for energetic purification of the incident beam, in the case that the source is, in practice, not yielding a perfectly monochromatic matter wave.

In accordance with our previous studies [24], we consider a double barrier potential of the form

$$V(x) = V_0[e^{-(x-x_1-L/2)^2/\sigma^2} + e^{-(x-x_1+L/2)^2/\sigma^2}], \tag{29}$$

with x_1 the central position between the two barriers, L the distance between the maxima, and σ the width of the barriers. The Bose-Einstein condensate is assumed to consist of ^{87}Rb atoms with the scattering length $a_{sc} = 5.77$ nm and to propagate in a waveguide with the transverse confinement frequency $\omega_\perp = 2\pi \times 10^3$ s^{-1}. In terms of $\omega_\perp$ and the transverse oscillator length $a_\perp = \sqrt{\hbar/m\omega_\perp} \simeq 0.34$ μm, we therefore have $g \simeq 0.034\hbar\omega_\perp a_\perp$. As in Ref. [24], we choose $V_0 = \hbar\omega_\perp$ and $L = 10\sigma = 5\,\mu\text{m} \simeq 14.7a_\perp$ for the parameters of the potential (29).

The main characteristics of this transport process can be understood on the level of the inhomogeneous Gross-Pitaevskii

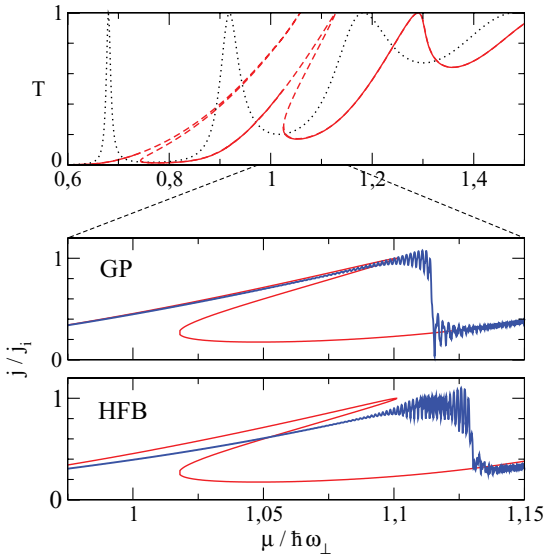

FIG. 2. (Color online) Time-dependent sweep across a resonance of the double barrier potential [Eq. (29)] (which is displayed in the lower panel of Fig. 3). The upper panel shows the nonlinear transmission spectrum at the incident current $j_i = 1.6\omega_\perp$ obtained from the integration of the Gross-Pitaevskii equation [Eq. (30)] with the interaction strength $g \simeq 0.034\hbar\omega_\perp a_\perp$. Dashed lines mark the resonance branches that are not directly accessible by means of a straightforward injection of matter waves at fixed chemical potential. The dotted line represents the linear transmission spectrum at $g = 0$. The middle and lower panels show the time-dependent transmission that is obtained by sweeping the chemical potential according to Eq. (31) during the propagation process. This sweep allows one to populate the upper branch of the resonance peak that corresponds to the fifth excited quasibound state within the cavity. Apart from a slight shift of the distorted resonance peak (due to a renormalization of the effective interaction strength), the calculation based on the dynamical Hartree-Fock–Bogoliubov (HFB) equations [Eqs. (19)–(21)] (lower panel) reproduces quite well the Gross-Pitaevskii (GP) calculation (middle panel).

equation

$$i\hbar\frac{\partial}{\partial t}\psi(x,t) = H_0^{(x)}\psi(x,t) + g\,|\psi(x,t)|^2\,\psi(x,t) + S(x,t)\exp(-i\mu t/\hbar), \tag{30}$$

which corresponds to the lowest-order truncation of the system of equations [Eqs. (19)–(21)]. The upper panel of Fig. 2 displays the transmission spectrum through this double barrier potential as a function of the condensate's chemical potential μ, in the absence and presence of the interaction between the atoms (dotted and solid-dashed lines, respectively), which is computed by means of stationary scattering solutions of the Gross-Pitaevskii equation that exhibit the incident current $j_i = 1.6\omega_\perp$. For a noninteracting condensate, a sequence of Breit-Wigner peaks would be obtained in the transmission, whose positions and widths correspond to the energies and decay rates, respectively, of the quasibound states within the resonator. These transmission peaks exist also in the presence of interaction, but become strongly distorted toward higher chemical potentials (for repulsive interaction) due to the nonlinearity in the Gross-Pitaevskii equation [24,26]. A multivalued transmission spectrum with several bistable branches is thereby obtained, which is typical for nonlinear transmission problems and arises also in nonlinear optics [31] as well as in the electronic transport through quantum wells [44–46].

It is easy to see that a direct, straightforward injection of matter waves onto this atomic Fabry-Perot resonator at a given chemical potential μ would always lead to the population of the lowest branch in the transmission spectrum [24,26]. Hence, resonant transmission through long-lived quasibound states with narrow widths cannot be achieved in this way, and the atomic quantum dot qualitatively acts like a simple potential barrier, giving rise to nearly perfect (classical-like) reflection of the condensate for chemical potentials well below the barrier height V_0. Indeed, if the chemical potential of the incident beam is chosen to match the level of an internal (noninteracting) quasibound state, a finite population of this state will shift the associated level toward higher energies, and the matter-wave beam will no longer be on resonance. On the other hand, injecting the condensate at the appropriate chemical potential that corresponds to the position of the *distorted* resonance peak would not yield any population in the internal quasibound state in the first place if the resonator was initially empty.

In Ref. [24] we proposed a control scheme that allows one to overcome this limitation and to achieve resonant transport of the condensate in the presence of finite interaction. The basic idea is that the chemical potential of the condensate (or, equivalently, the offset potential of the waveguide) needs to be adiabatically varied *during the propagation process*, in order to follow the upper branch of one of the distorted resonance peaks. The feasibility of this scheme was demonstrated through numerical simulations on the basis of the time-dependent Gross-Pitaevskii equation. Starting at a chemical potential on the left shoulder of the resonance peak corresponding to the fifth excited quasibound state (which is magnified in the middle and lower panels of Fig. 2), and increasing the chemical potential up to the value that equals the peak's top position, we obtained nearly perfect transmission on finite time scales, limited only by the dynamical instability of the nonlinear scattering state at resonance [24].

The middle and lower panels of Fig. 2 display the outcome of a similar time-dependent transport process, which was calculated here with the Gross-Pitaevskii equation (middle panel) as well as through the numerical integration of the dynamical Hartree-Fock–Bogoliubov equations [Eqs. (19)–(21)]. In these calculations, we first populated a scattering state at the chemical potential $\mu_0 = 0.97\hbar\omega_\perp$, by ramping up the source amplitude within the propagation time $t_0 = 10^3\omega_\perp^{-1}$, and then subjected it to a linear sweep of the chemical potential according to

$$\mu(t) = \mu_0 + (t - t_0)\dot{\mu}, \tag{31}$$

with $\dot{\mu} = 5 \times 10^{-5}\hbar\omega_\perp^2$. Both calculations lead to a similar scenario, namely the adiabatic population of the upper branch of the resonance peak corresponding to the fifth excited quasibound state in the resonator, and the subsequent decay to a low-transmission state at propagation times t at which the corresponding chemical potential $\mu(t)$ exceeds the position of the resonance peak.

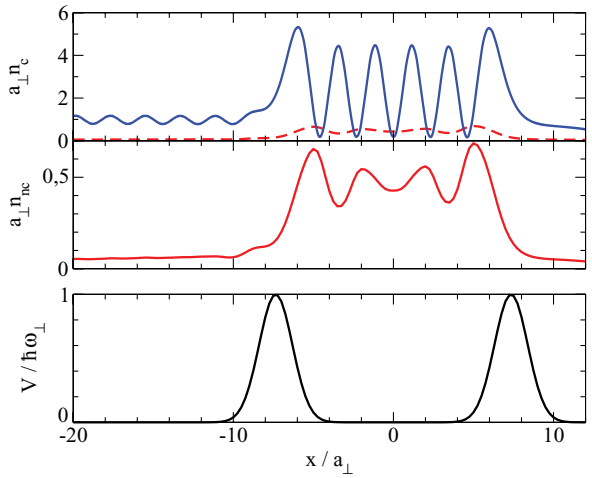

FIG. 3. (Color online) Density of the condensate wave function (upper panel) and of the noncondensed atoms (middle panel; also shown as red dashed line in the upper panel) near a resonance of the double barrier potential [Eq. (29)]. The plot represents a snapshot of the time-dependent sweep across the resonance shown in Fig. 2 at the evolution time at which the chemical potential equals $\mu = 1.1\hbar\omega_\perp$, corresponding to a transmission of $T \simeq 0.85$. The lower panel shows the double barrier potential.

A slight displacement in the peak position and in the slope of the resonance branch is observed in the HFB calculations when being compared with the nonlinear transmission curve obtained from the Gross-Pitaevskii equation. We attribute this to a renormalization of the effective nonlinearity strength in Eqs. (19)–(21) due to the coupling of the condensate wave function to the two-point functions $\Phi(x_1, x_2, t)$ and $\Gamma(x_1, x_2, t)$. This is explained in more detail in the Appendix, which also provides a quantitative reproduction of the displacement.

Figure 3 displays the condensate density (n_c) as well as the density of noncondensed atoms ($n_{\rm nc}$) of the instantaneous scattering state at the propagation time t with $\mu(t) = 1.1$ at which an overall transmission of $T \simeq 0.85$ is obtained. We clearly see a finite cloud of noncondensed atoms within the resonator, which is obviously induced by the large local density fluctuations of the condensate. The noncondensed density is found to slowly increase with time during the sweep of the chemical potential, but remains rather low compared to the condensate density on the time scales that are considered here.

Our study indicates that the control scheme proposed in Ref. [24] is working not only within the Gross-Pitaevskii description of the transport process, but remains feasible also from a more microscopic point of view taking into account the noncondensed cloud that is generated within the scattering region. We remark, however, that this conclusion strongly depends on the specific parameters at hand. Indeed, if we increase the microscopic interaction strength of the atoms by a factor of 2 (which could possibly be achieved through a Feshbach resonance) while keeping the other parameters of the system fixed, we find rather strong depletion of the condensate within the resonator during the time-dependent sweep of the chemical potential across the resonance. In this situation, the truncation scheme leading to Eqs. (19)–(21) would not be justified any longer, and we expect that at that particular high value of the interaction strength the overall coherence of the atomic cloud cannot be maintained and the condensate would become destroyed during the transport process.

IV. TRANSPORT THROUGH DISORDER POTENTIALS

Let us now consider the transport of Bose-Einstein condensates through disorder potentials of finite range, consisting of a more or less random sequence of several barriers and wells with different heights and depths. Such disorder potentials received special attention in previous years due to the possibility of realizing Anderson localization with ultracold atoms [5,6,47–51]. This task was ultimately achieved in two independent experiments [5,6] studying the expansion of condensates within optical speckle fields [5] as well as within bichromatic optical lattices [6], in a parameter regime where effects of the atom-atom interaction on the expansion process could be neglected. Indeed, various theoretical studies revealed that the presence of a finite nonlinearity in the wave equation that describes the expansion process, which would correspond to a finite interaction strength within the mean-field description of the condensate, would lead to a significant deviation from the scenario of Anderson localization, involving indefinite spreading of the tails of the condensate wave function instead of exponential localization [52–55].

The effect of a finite interaction is predicted to be even more dramatic in *scattering* processes through disorder potentials. Here, Anderson localization would manifest in an exponential decrease of the average transmission T with the spatial length L of the disorder region (or, more precisely, in a linear increase of the average $\langle -\ln T\rangle$ with L), which is induced by the destructive interference between multiply reflected components of the scattering wave function [56]. In the presence of a finite nonlinearity, however, a crossover to an *algebraic* decrease of the average transmission according to $\langle T\rangle \sim (L + L_0)^{-1}$ is encountered [25], which would essentially correspond to Ohm's law for incoherent transport. We find that this crossover is directly connected with the appearance of *permanently time-dependent scattering* of the condensate [25,57]. That is, the injection process of the condensate according to the working principle of the guided atom laser does not lead to the population of a quasistationary scattering state, but induces time-dependent fluctuations of the condensate density beyond a certain critical value of the source amplitude.

The main finding of our investigation of this problem with the kinetic Hartree-Fock–Bogoliubov equations [Eqs. (19)–(21)] is that the appearance of permanently time-dependent scattering within the Gross-Pitaevskii description of the transport process involves strong depletion and the production of a comparatively large cloud of noncondensed atoms. This indicates that the overall coherence characterizing the condensate becomes destroyed on a microscopic level, which would indeed be consistent with an Ohm-like scenario of incoherent transport through the disorder region. We exemplify this behavior with one particular, relatively short disorder potential, displayed in the lower panels of Figs. 4 and 5. For the chemical potential of the incident beam, we consider $\mu = 1.0\hbar\omega_\perp$, which is of the same order as the barrier heights of the disorder potential. As in Sec. III, we

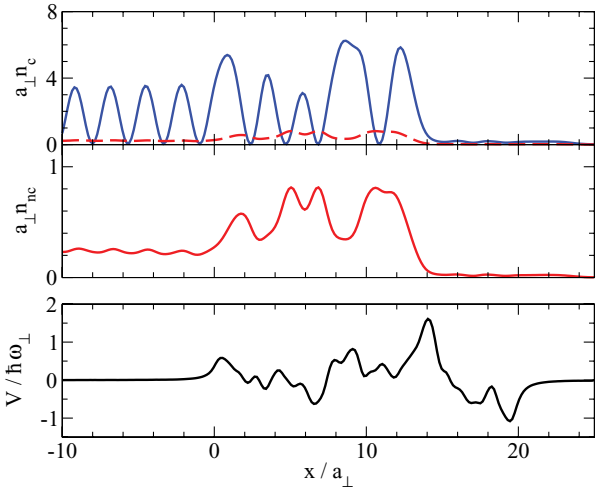

FIG. 4. (Color online) Density of the condensate wave function (upper panel) and of the noncondensed atoms (middle panel; also shown as red dashed line in the upper panel) during the time-dependent propagation process of the condensate through a disorder potential, at the evolution time $t = 1000/\omega_\perp$ (corresponding to 160 ms). The incident current $j_i = 1.5\omega_\perp$ was chosen such that a Gross-Pitaevskii calculation of the transport process yields a quasistationary scattering state. During the propagation process, noncondensed atoms are found to slowly accumulate preferably around the minima of the disorder potential, which is shown in the lower panel. The total depletion, however, is still relatively low at $t = 1000/\omega_\perp$.

choose $\omega_\perp = 2\pi \times 10^3$ s^{-1} for the transverse confinement frequency of the waveguide and $g = 0.034\hbar\omega_\perp a_\perp$ for the effective one-dimensional interaction strength.

Let us first consider the transport process across this disorder potential at the incident current $j_i = 1.5\omega_\perp$ for

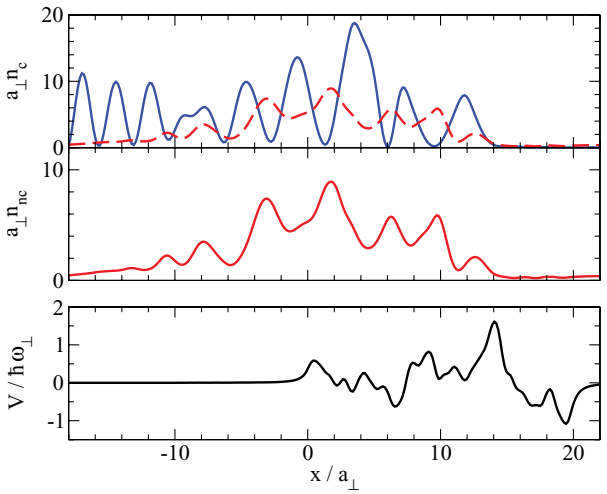

FIG. 5. (Color online) Same as Fig. 4 for a higher incident current $j_i = 4.775\omega_\perp$ for which the Gross-Pitaevskii calculation yields permanently time-dependent scattering. The figure shows a snapshot at the evolution time $t = 500/\omega_\perp$. Here the density of noncondensed atoms $n_{\rm nc}$ is of the same order as the condensate density, which indicates strong depletion and the destruction of the condensate on the microscopic level.

which a Gross-Pitaevskii calculation yields quasistationary scattering. At this relatively low value of the incident current, we find nearly stationary dynamics on the level of the kinetic Hartree-Fock–Bogoliubov equations [Eqs. (19)–(21)] as well, where the density of the scattering state is, as shown in Fig. 4, dominated by the coherent component associated with the condensate. As for the double barrier potential discussed in Sec. III, a finite, slowly increasing amount of depletion is generated within the scattering region, with noncondensed atoms preferably accumulating around the combined minima of the disorder potential and the condensate density. On time scales of the order of $1000\omega_\perp^{-1}$ corresponding to 160 ms, however, the total density of noncondensed atoms is still rather low compared to the condensate, which indicates that the coherence of the atomic beam should be well preserved also on the microscopic level.

The situation is rather different for a high incident current such as $j_i = 4.775\omega_\perp$, for which the simulation of the scattering process on the basis of the Gross-Pitaevskii equation yields permanently time-dependent fluctuations. Such time-dependent behavior is also found on the level of the kinetic Hartree-Fock–Bogoliubov equations [Eqs. (19)–(21)], together with a rather large amount of depletion, as shown by the snapshot displayed in Fig. 5. In that case, the truncation scheme leading to the closed system of Eqs. (19)–(21) can no longer be justified, and higher-order cumulants such as $\langle \delta\hat{\psi}(x_1,t)\delta\hat{\psi}(x_2,t)\delta\hat{\psi}(x_3,t)\rangle$, for instance, would have to be taken into account as well for an accurate description of the transport process. We conjecture that in this situation the condensate fraction becomes destroyed on a microscopic level, and the transport process becomes incoherent.

Figure 6 provides a comparison of the time-dependent currents of the condensate and the noncondensed atoms [cf. Eq. (24)] for the cases of low and high intensity of the incident matter-wave beam. Although a stable stationary flow, dominated by the coherent component of the condensate, is encountered in the presence of a low incident current, time-dependent dynamics arises already during the ramping process of the source for $j_i = 4.775\omega_\perp$ and induces, in turn, rather strong depletion from $\omega_\perp t \simeq 350$ on. Obviously, our calculation is, in this latter case, not trustable any longer beyond that evolution time as far as the accurate prediction of the time-dependent densities and currents of the condensate and the noncondensed fractions is concerned.

The scenario discussed here is also systematically found for a number of other disorder potentials of similar length as the one shown in Figs. 4 and 5. Stationary scattering on the Gross-Pitaevskii level implies, in general, a nearly stationary and fairly coherent flux on the level of the kinetic Hartree-Fock–Bogoliubov equations, whereas time-dependent scattering within the Gross-Pitaevskii equation leads to strong depletion. This is illustrated in Fig. 7, which shows the time evolution of the current of noncondensed atoms for 17 different, randomly generated disorder potentials that exhibit the same basic properties [i.e., the same average barrier height and the same correlation length (see Ref. [25] for more details)] as the potential of Figs. 4 and 5. These random potentials were selected such that they exhibit stable, time-independent flow on the level of the Gross-Pitaevskii equation for the incident current $j_i = 2.387\omega_\perp$. With one exception (dotted brown line)

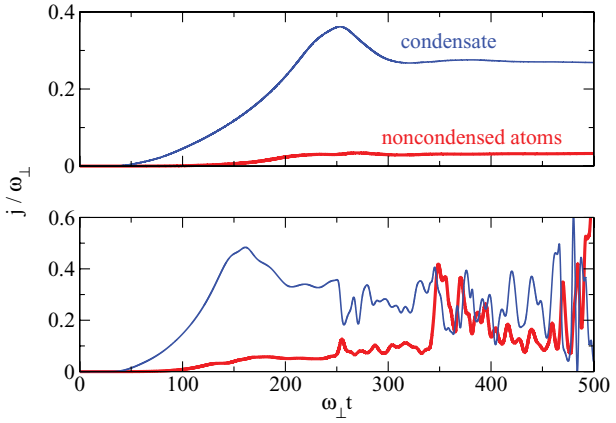

FIG. 6. (Color online) Total current of the condensate and the noncondensed atoms (narrow blue and wide red lines, respectively) as a function of the propagation time, for the incident currents $j_i = 1.5\omega_\perp$ (upper panel) and $j_i = 4.775\omega_\perp$ (lower panel), in the presence of the disorder potential that is shown in Fig. 4. The plots include the time interval of the initial ramping process of the source amplitude, which lasts until $t \simeq 300/\omega_\perp$. In the case of a rather low incident current (upper panel) for which a Gross-Pitaevskii calculation would yield quasistationary transport, depletion remains rather low on finite time scales. At higher incident currents for which permanently time-dependent scattering manifests on the Gross-Pitaevskii level, we find strongly enhanced depletion and a current of noncondensed atoms that is comparable to the current of the condensate fraction. This indicates, on a microscopic level, that the condensate becomes destroyed during this time-dependent scattering process.

stable flow is also found with our Hartree-Fock–Bogoliubov approach, and with two more exceptions [violet (top) and light-blue dashed lines] depletion in the transmitted current remains below 20% within the considered time interval $0 < \omega_\perp t < 1300$.

As a matter of fact, there is no rigorous one-to-one relation between stability on the Gross-Pitaevskii level and low

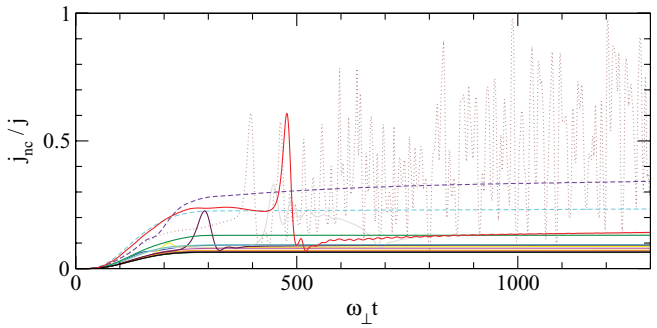

FIG. 7. (Color online) Relative current of noncondensed atoms (normalized by the total current) as a function of time for 17 different disorder potentials, at the incident current $j_i = 2.387\omega_\perp$. The disorder potentials were randomly generated and selected such that a stable, time-independent current is observed on the level of the Gross-Pitaevskii equation. With one exception (brown dotted line) stable flow is also found with our Hartree-Fock–Bogoliubov approach, and with two more exceptions [violet (top) and light-blue dashed lines] depletion in the transmitted current remains below 20% within the considered time interval.

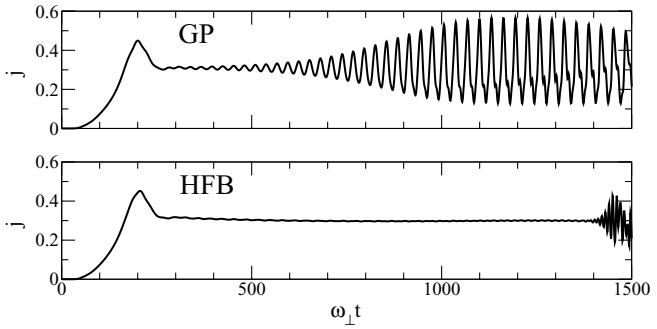

FIG. 8. Total atomic current across the disorder potential as a function of time, calculated for the critical incident current $j_i = 2.387\omega_\perp$ at which time-dependent scattering begins to appear on the level of the Gross-Pitaevkii equation (upper panel). A simulation of this scattering process with the kinetic Hartree-Fock–Bogoliubov equations (lower panel), however, yields quasistationary behavior on a time scale of the order of $1000\omega_\perp^{-1}$, with a reasonably low amount of depletion (between 15% and 20% of the total density), while dynamical instability and strong depletion sets in at $\omega_\perp t \simeq 1500$.

depletion on the Hartree-Fock–Bogoliubov level. Exceptions from this general equivalence particularly arise if the incident current of the condensate is close to the critical value $j_i^{(c)}$ beyond which permanently time-dependent scattering occurs on the level of the Gross-Pitaevskii equation. In this case, a small modification of the effective nonlinearity, caused by the coupling to the noncondensed cloud, can have a drastic effect and may destabilize—or, in some cases, also restabilize—the flow of the condensate. An example of this latter phenomenon is shown in Fig. 8 where the time evolution of the current across the disorder potential of Figs. 4 and 5 is shown for the incident current $j_i = 2.387\omega_\perp$, which is slightly larger than the critical incident current for destabilization on the Gross-Pitaevskii level. In contrast to the Gross-Pitaevskii calculation, the simulation of this transport process with the kinetic Hartree-Fock–Bogoliubov equations does not give rise to time-dependent fluctuations of the current on time scales of the order of $1000\omega_\perp^{-1}$ (which would correspond to 160 ms) and leads to a stable flux with a reasonably low amount of depletion, until destabilization sets in later on at $\omega_\perp t \simeq 1500$.

V. CONCLUSION

In this work, we investigated the transport of guided bosonic matter waves through one-dimensional scattering potentials by means of the inhomogeneous Hartree-Fock–Bogoliubov equations, which simulate the coherent injection of those matter waves from a trapped Bose-Einstein condensate [12]. A straightforward numerical integration of these Hartree-Fock–Bogoliubov equations yields nearly stationary, mean-field-like scattering dynamics of the bosonic flow on reasonably long time scales, provided the effective one-dimensional interaction strength is not too large and the integration of the corresponding Gross-Pitaevskii equation leads to quasistationary scattering. In that case, a comparatively low amount of depletion is obtained, with noncondensed atoms preferably accumulating around the local minima of the scattering potential. If, on the other hand, the nonlinear scattering dynamics of the

condensate is explicitly time-dependent on the level of the Gross-Pitaevskii equation, we encounter strong depletion and a rather large density of noncondensed atoms within the Hartree-Fock–Bogoliubov description. This indicates that the condensate becomes destroyed on a microscopic many-body description of the transport process, and that the atoms are individually propagating across the scattering potential.

It would be interesting, although beyond the scope of this work, to compare our findings with the truncated Wigner approach [58–61], which represents an alternative method to describe dynamical transport processes of Bose-Einstein condensates beyond the Gross-Pitaevskii description. In this approach, the microscopic quantum dynamics of the atomic cloud is described by a set of classical fields that sample the distribution of the initial many-body state describing the Bose gas under consideration, and that evolve according to the time-dependent Gross-Pitaevskii equation. In our situation, this initial state would correspond to an almost-perfect Bose-Einstein condensate of the "reservoir" atoms that are confined in the three-dimensional magnetic trap. The classical fields that would have to be used for the truncated Wigner approach would therefore be rather similar at the initial stage of the matter-wave injection process; deviations between them, which ultimately give rise to a loss of coherence, should mainly arise in the presence of strongly time-dependent scattering where the occurrence of classical chaos in the Gross-Pitaevskii equation might induce an exponential sensitivity of the time evolution with respect to initial conditions. This would be consistent with our observation that depletion is particularly strong in the regime of permanently time-dependent scattering.

An interesting study in this context was recently reported in Ref. [62], where the quantitative amount of depletion was computed for a homogeneously moving three-dimensional condensate (initially defined as a plane wave in a box with periodic boundaries) in the presence of an obstacle or a disorder potential. Using the truncated Wigner method, the authors showed that nonstationary, turbulent flow of the condensate leads to rather rapid depletion, on time scales that seem to be roughly comparable with our investigations [63]. Good agreement between the time-dependent Hartree-Fock–Bogoliubov approach and the truncated Wigner approach was, moreover, reported in other studies [64] that were focusing on collapsing Bose-Einstein condensates.

We finally point out again that several idealizations and approximations were employed for the description of the bosonic transport process. Specifically, we assumed an infinitely large condensate in the reservoir, which is perfectly coherent and which is not significantly depopulated during the outcoupling process. Ultracold Bose gases in realistic traps, however, do exhibit a finite number of noncondensed atoms in their many-body ground state, which should have an additional influence on the transport process. Clearly, the truncated Wigner method appears most suited in order to evaluate the effect of such initial quantum fluctuations.

Furthermore, we neglected the population of transversally excited modes in the waveguide, which should indeed play a role for the parameters of the waveguide and the scattering potentials that we considered in our study [65]. We also excluded nonlinear backaction with the source by making the idealizing assumption that the interaction strength of the waveguide atoms is negligible in the vicinity of the magnetic trap. These simplifications would have to be reconsidered for the simulation of a realistic matter-wave propagation experiment based on an atom laser. We do, however, not expect that the general findings obtained in this study would qualitatively alter if these complications are properly taken into account.

ACKNOWLEDGMENTS

We are grateful to Thomas Gasenzer, David Hutchinson, Gora Shlyapnikov, and Sebastian Wüster for enlightening discussions. T. Paul gratefully acknowledges funding from the Excellence Initiative of the German Research Foundation (DFG) through the Heidelberg Graduate School of Fundamental Physics (Grant No. GSC 129/1), the Global Networks Mobility Measures of the Frontier Innovation Fund of the University of Heidelberg, and the Alexander von Humboldt Foundation. P. Schlagheck acknowledges support through the DFG Forschergruppe FOR760.

APPENDIX: SINGLE-MODE DESCRIPTION OF RESONANT TRANSPORT WITH DEPLETION

In this appendix, we present a simple model that qualitatively explains the displacement of the distorted resonance peak in the lower panel of Fig. 2. We assume for this purpose that near the resonance only one of the quasibound states within the double barrier potential is involved in the transmission process. We denote the wave function of this state by $\chi_n(x)$, its energy by E_n, and its decay rate, corresponding to the full width at half-maximum (FWHM) of the resonance peak, by γ_n.

Generalizing the treatment in Ref. [26], we make the ansatz

$$\psi(x,t) \equiv \psi_n(t)\chi_n(x)e^{-i\mu t/\hbar}, \tag{A1}$$

$$\phi(x_1,x_2,t) \equiv \phi_{nn}(t)\chi_n(x_1)\chi_n(x_2)e^{-2i\mu t/\hbar}, \tag{A2}$$

$$\Gamma(x_1,x_2,t) \equiv \Gamma_{nn}(t)\chi_n(x_1)\chi_n(x_2), \tag{A3}$$

and insert it into Eqs. (19)–(21). Neglecting contributions of the order $O(N^{-1})$, we obtain

$$i\hbar\frac{\partial}{\partial t}\psi_n = \left(E_n - \frac{i}{2}\gamma_n - \mu + g_n|\psi_n|^2\right)\psi_n + 2g_n\Gamma_{nn}\psi_n + g_n\phi_{nn}\psi_n^* + S_n, \tag{A4}$$

$$i\hbar\frac{\partial}{\partial t}\phi_{nn} = (2E_n - i\gamma_n - 2\mu + 4g_n|\psi_n|^2)\phi_{nn} + 2g_n\psi_n^2\Gamma_{nn} + g_n\psi_n^2, \tag{A5}$$

$$i\hbar\frac{\partial}{\partial t}\gamma_{nn} = -i\gamma_n\Gamma_{nn} + g_n\left(\psi_n^2\phi_{nn}^* - (\psi_n^*)^2\phi_{nn}\right), \tag{A6}$$

where we have introduced the effective source amplitude S_n and the effective nonlinearity $g_n \equiv g\int dx|\chi_n(x)|^4$ associated with the state $\chi_n(x)$. Assuming that a stationary scattering state is realized, we set the time derivatives on the left-hand sides of Eqs. (A4)–(A6) equal to zero. Equation (21) is then solved as

$$\Gamma_{nn} = \frac{g_n}{i\gamma_n}\left(\psi_n^2\phi_{nn}^* - (\psi_n^*)^2\phi_{nn}\right). \tag{A7}$$

We are now interested in estimating the shift of the distorted resonance structure due to the admixture of ϕ_{nn} and Γ_{nn} in Eq. (A4). For this purpose, we set the chemical potential equal to the top of the "unperturbed" resonance peak obtained within the Gross-Pitaevskii equation, that is

$$\mu = E_n + g_n|\psi_n|^2, \tag{A8}$$

where $|\psi_n|^2 = 4|S_n|^2/\gamma_n^2$ is the maximal population of the quasibound state at the top of the peak. Inserting the expressions (A7) and (A8) into Eq. (A5) yields

$$\left(g_n|\psi_n|^2 - \frac{i}{2}\gamma_n + i\frac{g_n^2}{\gamma_n}|\psi_n|^4\right)\phi_{nn} - i\frac{g_n^2}{\gamma_n}\psi_n^4\phi_{nn}^* + \frac{1}{2}g_n\psi_n^2 = 0\,. \tag{A9}$$

This equation is explicitly solved with

$$\phi_{nn} = -\frac{2g_n}{\gamma_n^2}\psi_n^2\left(g_n|\psi_n|^2 + \frac{i}{2}\gamma_n\right), \tag{A10}$$

which in turn implies

$$\Gamma_{nn} = 2\frac{g_n^2}{\gamma_n^2}|\psi_n|^4\,. \tag{A11}$$

Inserting these expressions (A10) and (A11) into Eq. (A4) finally gives rise to

$$\left(E_n - \frac{i}{2}\gamma_n - \mu + g_n^{(\mathrm{eff})}|\psi_n|^2\right)\psi_n + S_n = 0, \tag{A12}$$

with the renormalized (complex) nonlinearity parameter

$$g_n^{(\mathrm{eff})} \equiv \left(1 + 2\frac{g_n^2}{\gamma_n^2}|\psi_n|^2 - i\frac{g_n}{\gamma_n}\right)g_n\,. \tag{A13}$$

For a quantitative comparison with the shift of the resonance peak in the lower panel of Fig. 2, we need to take into account the fact that the rate γ_n that describes the decay of the quasibound state χ_n strongly depends on the population of this state, due to the the presence of the nonlinearity (see also the discussion in Ref. [26]). In lowest order, γ_n can be estimated by the decay rate of a (fictitious) quasibound state of the noninteracting system whose energy equals the chemical potential of the distorted resonance peak. The latter appears, in our case, at $\mu \simeq 1.1\hbar\omega_\perp$. From the upper panel of Fig. 2, we can, with this reasoning, approximately extract $\gamma_n \simeq 0.1\hbar\omega_\perp$. We furthermore infer $g_n|\psi_n|^2 \simeq 0.2\hbar\omega_\perp$, which corresponds to the distortion of the peak position with respect to the linear system.

Approximating the wave function of the quasibound state by $\chi_n(x) = \sqrt{2/L}\sin(n\pi x/L)$, which would result from sharp and infinitely high barriers with distance L, we obtain $\int_0^L dx|\chi_n(x)|^4 = 1.5L$. Using $L \simeq 14.7a_\perp$ and $g \simeq 0.034\hbar\omega_\perp a_\perp$, this yields $g_n = 1.5g/L \simeq 0.003\hbar\omega_\perp$. Altogether, we therefore obtain the estimate

$$\Re\left(g_n^{(\mathrm{eff})} - g_n\right)|\psi_n|^2 = 2g_n\frac{g_n^2|\psi_n|^4}{\gamma_n^2} \simeq 0.025\hbar\omega_\perp, \tag{A14}$$

for the shift of the resonance peak. This is indeed in fairly good agreement with the numerically computed shift shown in Fig. 2, which is also of the order of $0.025\hbar\omega_\perp$.

[1] R. Dumke, T. Müther, M. Volk, W. Ertmer, and G. Birkl, Phys. Rev. Lett. **89**, 220402 (2002).

[2] R. Folman, P. Krüger, D. Cassettari, B. Hessmo, T. Maier, and J. Schmiedmayer, Phys. Rev. Lett. **84**, 4749 (2000).

[3] W. Hänsel, P. Hommelhoff, T. W. Hänsch, and J. Reichel, Nature **413**, 498 (2001).

[4] J. Fortágh and C. Zimmermann, Rev. Mod. Phys. **79**, 235 (2007).

[5] J. Billy, V. Josse, Z. Zuo, A. Bernard, B. Hambrecht, P. Lugan, D. Clément, L. Sanchez-Palencia, P. Bouyer, and A. Aspect, Nature **453**, 891 (2008).

[6] G. Roati, C. D'Errico, L. Fallani, M. Fattori, C. Fort, M. Zaccanti, G. Modugno, M. Modugno, and M. Inguscio, Nature **453**, 895 (2008).

[7] T. Campey, C. J. Vale, M. J. Davis, N. R. Heckenberg, H. Rubinsztein-Dunlop, S. Kraft, C. Zimmermann, and J. Fortágh, Phys. Rev. A **74**, 043612 (2006).

[8] H. Ott, J. Fortágh, S. Kraft, A. Günther, D. Komma, and C. Zimmermann, Phys. Rev. Lett. **91**, 040402 (2003).

[9] J. E. Lye, L. Fallani, C. Fort, V. Guarrera, M. Modugno, D. S. Wiersma, and M. Inguscio, Phys. Rev. A **75**, 061603(R) (2007).

[10] M.-O. Mewes, M. R. Andrews, D. M. Kurn, D. S. Durfee, C. G. Townsend, and W. Ketterle, Phys. Rev. Lett. **78**, 582 (1997).

[11] I. Bloch, T. W. Hänsch, and T. Esslinger, Phys. Rev. Lett. **82**, 3008 (1999).

[12] W. Guerin, J.-F. Riou, J. P. Gaebler, V. Josse, P. Bouyer, and A. Aspect, Phys. Rev. Lett. **97**, 200402 (2006).

[13] J. Billy, V. Josse, Z. Zuo, W. Guerin, A. Aspect, and P. Bouyer, Ann. Phys. (Paris) **32**, 17 (2007).

[14] J.-F. Riou, Y. Le Coq, F. Impens, W. Guerin, C. J. Bordé, A. Aspect, and P. Bouyer, Phys. Rev. A **77**, 033630 (2008).

[15] A. Couvert, M. Jeppesen, T. Kawalec, G. Reinaudi, R. Mathevet, and D. Guéry-Odelin, EPL **83**, 50001 (2008).

[16] D. K. Ferry and S. M. Goodnick, *Transport in Nanostructures* (Cambridge University Press, Cambridge, 1997).

[17] J. H. Thywissen, R. M. Westervelt, and M. Prentiss, Phys. Rev. Lett. **83**, 3762 (1999).

[18] I. Carusotto and G. C. La Rocca, Phys. Rev. Lett. **84**, 399 (2000).

[19] I. Carusotto, Phys. Rev. A **63**, 023610 (2001).

[20] P. Leboeuf and N. Pavloff, Phys. Rev. A **64**, 033602 (2001).

[21] P. Leboeuf, N. Pavloff, and S. Sinha, Phys. Rev. A **68**, 063608 (2003).

[22] K. Rapedius, D. Witthaut, and H. J. Korsch, Phys. Rev. A **73**, 033608 (2006).

[23] K. Rapedius and H. J. Korsch, Phys. Rev. A **77**, 063610 (2008).

[24] T. Paul, K. Richter, and P. Schlagheck, Phys. Rev. Lett. **94**, 020404 (2005).

[25] T. Paul, P. Leboeuf, N. Pavloff, K. Richter, and P. Schlagheck, Phys. Rev. A **72**, 063621 (2005).

[26] T. Paul, M. Hartung, K. Richter, and P. Schlagheck, Phys. Rev. A **76**, 063605 (2007).
[27] C. Menotti and S. Stringari, Phys. Rev. A **66**, 043610 (2002).
[28] M. Girardeau, J. Math. Phys. **1**, 516 (1960).
[29] M. Olshanii, Phys. Rev. Lett. **81**, 938 (1998).
[30] D. S. Petrov, G. V. Shlyapnikov, and J. T. M. Walraven, Phys. Rev. Lett. **85**, 3745 (2000).
[31] R. W. Boyd, *Nonlinear Optics* (Academic Press, London, 1992).
[32] N. P. Proukakis and K. Burnett, J. Res. Natl. Inst. Stand. Technol. **101**, 457 (1996).
[33] T. Köhler and K. Burnett, Phys. Rev. A **65**, 033601 (2002).
[34] D. A. W. Hutchinson, K. Burnett, R. J. Dodd, S. A. Morgan, M. Rusch, E. Zaremba, N. P. Proukakis, M. Edwards, and C. W. Clark, J. Phys. B **33**, 3825 (2000).
[35] A. Griffin, Phys. Rev. B **53**, 9341 (1996).
[36] We remark that it is possible to formulate Hartree-Fock–Bogoliubov approaches that preserve the gauge symmetry of the Bose gas;see S. A. Gardiner and S. A. Morgan, Phys. Rev. A **75**, 043621 (2007).
[37] E. H. Lieb, R. Seiringer, and J. Yngvason, Rep. Math. Phys. **59**, 389 (2007).
[38] M. Jääskeläinen and S. Stenholm, Phys. Rev. A **66**, 023608 (2002).
[39] E. H. Lieb, R. Seiringer, and J. Yngvason, Phys. Rev. A **61**, 043602 (2000).
[40] W. H. Press, S. A. Teukolsky, W. T. Vetterling, and B. P. Flannery, *Numerical Recipes* (Cambridge University Press, Cambridge, 1986).
[41] E. Cerboneschi, R. Mannella, E. Arimondo, and L. Salasnich, Phys. Lett. **A249**, 495 (1998).
[42] R. Kosloff and D. Kosloff, J. Comput. Phys. **63**, 363 (1986).
[43] N. Moiseyev, L. D. Carr, B. A. Malomed, and Y. B. Band, J. Phys. B **37**, L193 (2004).
[44] V. J. Goldman, D. C. Tsui, and J. E. Cunningham, Phys. Rev. Lett. **58**, 1256 (1987).
[45] C. Presilla, G. Jona-Lasinio, and F. Capasso, Phys. Rev. B **43**, 5200 (1991).
[46] M. Y. Azbel', Phys. Rev. B **59**, 8049 (1999).
[47] D. Clément, A. F. Varón, M. Hugbart, J. A. Retter, P. Bouyer, L. Sanchez-Palencia, D. M. Gangardt, G. V. Shlyapnikov, and A. Aspect, Phys. Rev. Lett. **95**, 170409 (2005).
[48] C. Fort, L. Fallani, V. Guarrera, J. E. Lye, M. Modugno, D. S. Wiersma, and M. Inguscio, Phys. Rev. Lett. **95**, 170410 (2005).
[49] T. Schulte, S. Drenkelforth, J. Kruse, W. Ertmer, J. Arlt, K. Sacha, J. Zakrzewski, and M. Lewenstein, Phys. Rev. Lett. **95**, 170411 (2005).
[50] L. Sanchez-Palencia, D. Clément, P. Lugan, P. Bouyer, G. V. Shlyapnikov, and A. Aspect, Phys. Rev. Lett. **98**, 210401 (2007).
[51] S. E. Skipetrov, A. Minguzzi, B. A. van Tiggelen, and B. Shapiro, Phys. Rev. Lett. **100**, 165301 (2008).
[52] D. L. Shepelyansky, Phys. Rev. Lett. **70**, 1787 (1993).
[53] T. Kottos and M. Weiss, Phys. Rev. Lett. **93**, 190604 (2004).
[54] A. S. Pikovsky and D. L. Shepelyansky, Phys. Rev. Lett. **100**, 094101 (2008).
[55] G. Kopidakis, S. Komineas, S. Flach, and S. Aubry, Phys. Rev. Lett. **100**, 084103 (2008).
[56] P. W. Anderson, D. J. Thouless, E. Abrahams, and D. S. Fisher, Phys. Rev. B **22**, 3519 (1980).
[57] T. Paul, P. Schlagheck, P. Leboeuf, and N. Pavloff, Phys. Rev. Lett. **98**, 210602 (2007).
[58] C. Gardiner and P. Zoller, *Quantum Noise* (Springer, Berlin, 2004), 3rd ed.
[59] M. J. Steel, M. K. Olsen, L. I. Plimak, P. D. Drummond, S. M. Tan, M. J. Collett, D. F. Walls, and R. Graham, Phys. Rev. A **58**, 4824 (1998).
[60] A. Sinatra, C. Lobo, and Y. Castin, Phys. Rev. Lett. **87**, 210404 (2001).
[61] P. B. Blakie, A. S. Bradley, M. J. Davis, R. J. Ballagh, and C. W. Gardiner, Adv. Phys. **57**, 363 (2008).
[62] R. G. Scott and D. A. W. Hutchinson, Phys. Rev. A **78**, 063614 (2008).
[63] In Ref. [62], the characteristic time scale for the loss of coherence was found to be of the order of 1 ms, which is smaller compared to our findings. We attribute this to the considerably larger three-dimensional atomic densities that were considered in Ref. [62].
[64] S. Wüster, B. J. Dąbrowska-Wüster, A. S. Bradley, M. J. Davis, P. B. Blakie, J. J. Hope, and C. M. Savage, Phys. Rev. A **75**, 043611 (2007).
[65] Especially disorder potentials with deep attractive wells should allow for local transitions into the first excited transverse mode with radial symmetry, requiring an excitation energy of $2\hbar\omega_\perp$.